Research Article

Qahtan Adnan Abed*, Viorel Badescu, Adrian Ciocanea, Iuliana Soriga and Dorin Bureţea

Models for New Corrugated and Porous Solar Air Collectors under Transient Operation

DOI 10.1515/jnet-2016-0013
Received February 29, 2016; revised June 19, 2016; accepted July 13, 2016

Abstract: Mathematical models have been developed to evaluate the dynamic behavior of two solar air collectors: the first one is equipped with a V-porous absorber and the second one with a U-corrugated absorber. The collectors have the same geometry, cross-section surface area and are built from the same materials, the only difference between them being the absorbers. V-corrugated absorbers have been treated in literature but the V-porous absorbers modeled here have not been very often considered. The models are based on first-order differential equations which describe the heat exchange between the main components of the two types of solar air heaters. Both collectors were exposed to the sun in the same meteorological conditions, at identical tilt angle and they operated at the same air mass flow rate. The tests were carried out in the climatic conditions of Bucharest (Romania, South Eastern Europe). There is good agreement between the theoretical results and experiments. The average bias error was about 7.75 % and 10.55 % for the solar air collector with "V"-porous absorber and with "U"-corrugated absorber, respectively. The collector based on V-porous absorber has higher efficiency than the collector with U-corrugated absorber around the noon of clear days. Around sunrise and sunset, the collector with U-corrugated absorber is more effective.

Keywords: solar air collector, porous absorber, corrugated absorber, mathematical model, dynamic operation

1 Introduction

Solar air heaters are solar collectors which utilize air as working fluid. Widespread applications include space heating and drying processes. Among their advantages are simple maintenance and manufacturing, the fact that they do not freeze and are less prone to corrosion compared with solar water collectors. Solar air collectors can be glazed or unglazed, and their absorbers usually consist of materials having high solar absorbance and low emittance, i. e. selective characteristics.

Many researchers focused on the improvement of the thermal performance of solar air collectors. In order to enhance the heat transfer by convection from the absorber to the flowing air, several design solutions have been tested, such as corrugated absorber plate [1, 2], roughness geometry [3, 4] or fins welded over and under the absorber plate [5, 6]. The performance of a single-pass solar air heater with baffles was studied in [7]. The results show that increasing the number of fins and increasing the baffle

***Corresponding author: Qahtan Adnan Abed,** Engineering Technical College, Al-Furat Al-Awsat Technical University, Najaf, Iraq; Polytechnic University of Bucharest, Bucharest, Romania, E-mail: qahtan77@yahoo.com
Viorel Badescu, Candida Oancea Institute, Polytechnic University of Bucharest, Splaiul Independentei 313, Bucharest 060042, Romania; Romanian Academy, Calea Victoriei 125, Bucharest, Romania, E-mail: badescu@theta.termo.pub.ro
Adrian Ciocanea, Department of Hydraulic, Hydraulic Machinery and Environmental Engineering, Universitatea Politehnica din Bucuresti, Splaiul Independentei 313, Bucharest 060042, Romania, E-mail: adrian.ciocanea@upb.ro
Iuliana Soriga, Department of Thermotechnics, Engines, Thermal and Refrigeration Equipment, Universitatea Politehnica din Bucuresti, Splaiul Independentei, 313, Bucuresti 060042, Romania, E-mail: iulia.soriga@upb.ro
Dorin Bureţea, Department of Telematics and Electronics for Transports, Faculty of Transports, Polytechnic University of Bucharest, Splaiul Independentei 313, Bucharest 060042, Romania

width are effective at low mass flow rates. The thermal performance of a solar air collector with a fin fixed on the absorber has been studied in [8]. The authors found a bias error of 3.5 % between the theoretical and experimental results. The effect of geometrical parameters of circular transverse ribs on the heat transfer of a rectangular duct with heated plate has been studied in [9]. The thermal efficiency of a roughened duct is observed to be 5–9 % higher than that of a smooth duct.

There are two common absorber geometries of solar air collectors; the first one is the U-corrugated absorber and the second one is the V-corrugated absorber.

The convective heat transfer in U-corrugated solar collectors (see Figure 1) was studied numerically by Gao et al. [10]. The results show that, in order to efficiently suppress heat loss caused by natural convection, the height ratio should be greater than 2, the geometrical ratio should be greater than 1 and the angle of inclination should be less than 40°. The main objective of using U-corrugated absorbing plates is to enhance the turbulence and the heat transfer rate inside the air flow channel, both of which are crucial in improving the solar air collector efficiency [11, 12].

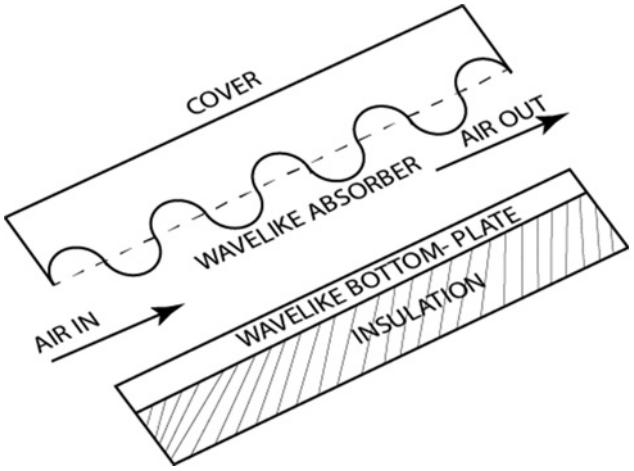

Figure 1: Schematic view of the cross-sectional area in a U-corrugated solar air heater [10].

A large number of studies have also been carried out on the V-corrugated solar air collector. Ref. [13] developed a mathematical model for such a collector. This model was able to correctly predict the mean temperature of all components of the collector, the instantaneous air temperature at any section of the collector, the output air temperature and the thermal conversion efficiency. It has been found that the best solar air collector with V-corrugated absorber plate has a height of 50 mm from the center of the triangle and a 60° tilt angle for the sides. This is shown in Figure 2.

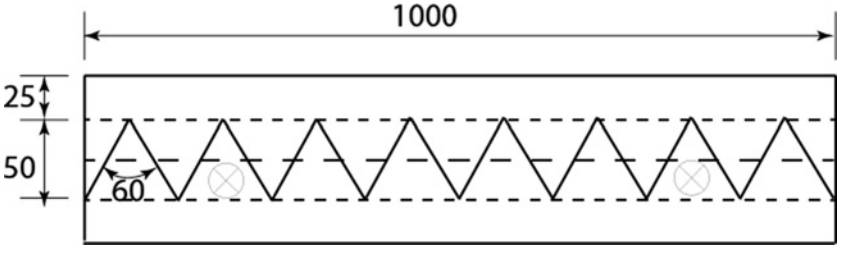

Figure 2: Design of an air collector with V-corrugated absorber [13].

The authors of Ref. [14] carried out experimental studies on the heat transfer characteristics and the performance of solar air collectors with rectangular fins. Solar air collectors with longitudinal rectangular fins array exhibited high thermal efficiency, which is attributed to the additional surface area. The thermal performance of V-groove and cross-corrugated solar air collectors had been compared theoretically in Ref. [15], under a wide range of configurations and operating conditions. The results showed that the cross-corrugated collector is superior to

the V-groove collector. The fabrication and performance evaluation of a V-groove solar air heater has been studied in [16]. The authors reported collector efficiency about 35 %.

Several studies have been performed on the performance of solar air collectors with porous absorbers. The authors of Refs. [17–19] investigated experimentally a single-pass solar air heater. The results showed that the efficiency of this solar air collector is higher than that of the solar air collector without porous media.

Trying to improve the thermal efficiency of solar thermal collectors, Munuswamy et al. [20] conducted numerical experiments on the effectiveness of nanoparticles in solar water collector systems. The authors of Ref. [21] studied theoretically and experimentally the performance of solar water heaters, in different operating conditions. The maximum thermal efficiency was about 45 %. Two flat plate collectors with the same surface area have been compared in [22]. The first one has internally grooved fins riser tubes and the second has plain riser tubes. The results show that the efficiency of the collector with finned tube is higher than that of the collector without riser tubes.

V-corrugated absorbers have been treated in several papers [13–16]. The novelty of this work is that it focuses on V-porous absorbers, which have been rarely considered in literature. The thermal performance of a collector with "V"-corrugated porous absorber is compared with that of a single-pass collector with "U"-corrugated absorber. The collectors are nearly identical since they differ only by the absorber type. The collectors are tested outdoor under the same meteorological and radiometric conditions. Transient mathematical models for these two types of solar air heaters are presented. The proposed models are of general interest as they can be easily used with different shapes of absorbers through changes in the criterial equation of the convection heat transfer coefficient. Validation is an important step in mathematical modeling development, and therefore comparisons with actual experimental results obtained at Bucharest – Romania (latitude 44°26′N, longitude 26°6′E) have been reported.

2 Experimental equipment

Both solar air collectors consist of absorber, glazing, insulation and a wood collector frame on which these components were assembled. Both collectors have a single glass cover (1.5 m × 0.75 m). The back and edges of both collectors are insulated with polystyrene in order to avoid heat losses. Two types of absorbers were used. The first one (the V-corrugated porous absorber) was made of soft steel with two layers of mesh wire while the second one (the U-corrugated absorber) was made of aluminum. The size of the two collectors is 1.52 m × 0.7 m × 0.0007 m and 1.4 m × 1.13 m × 0.00035 m, respectively. Table 1 presents the parameters of the collectors.

The two solar collectors were installed at the Polytechnic University of Bucharest (44°26′N, 26°6′E). The collectors' slope was 55°, which is adequate for space heating during winter at the geographical location of Bucharest.

A Kipp and Zonen CMP3 Pyranometer was used for measuring solar irradiance at the level and inclination of the collectors. The pyranometer was connected to a computer and the measurements were recorded at time intervals of 10 s.

A photograph and schematic view of the experimental setup are shown in Figure 3. The experimental studies were conducted during September and October 2014 under clear sky conditions. Further details are as follows.

2.1 Absorbers

The main component of solar air collectors is the absorber, which converts solar energy into heat and transfers it to the flowing air. The shape of the absorber is of significant importance. Moreover, increasing the absorber surface area increases the amount of heat transferred to the air [5, 6].

Table 1: Parameters of solar air collectors.

Parameters	Value	Unit
Collector		
Collector absorber area	1.125	m^2
Height of the collector	0.085	m
Transmittance of the glass cover	0.85	
Absorptance of the absorber	0.9	
V-corrugated porous absorber		
Absorber	Soft steel	
Absorber emissivity	0.8	
Absorber thickness	0.0007	m
Absorber density	7,820	kg/m^3
Absorber layers	2	
Absorber conductivity	15	W/(m K)
Specific heat of soft steel	502.4	J/(kg K)
"U"-corrugated absorber		
Absorber plate	Aluminum	
Absorber plate emissivity	0.1	
Absorber plate thickness	0.0007	m
Absorber plate density	2,700	kg/m^3
Absorber plate layers	1	
Absorber plate conductivity	237	W/(m K)
Specific heat of aluminum	904	J/(kg K)
Glass cover		
Number of transparent covers	1	
Transparent cover absorptance	0.2	

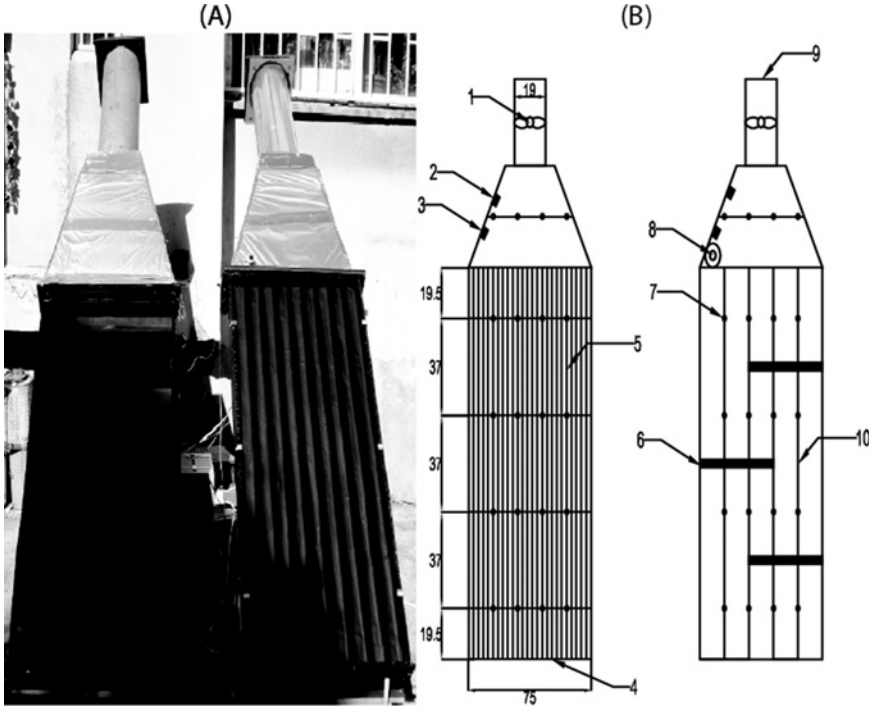

Figure 3: (A) photograph and (B) schematic view of the solar air collectors: (1) air fan, (2) humidity transducer, (3) pressure transducer, (4) air inlet, (5) V-corrugated porous absorber, (6) fins, (7) thermal transducer, (8) pyranometer, (9) air outlet and (10) "U"-corrugated absorber.

The absorbers of the collectors used in this study have different configurations and are made of different materials (see Figure 4). One collector is a single-passage air collector with the absorber made of aluminum ("U"-corrugated absorber). The other collector is an original through-pass air collector with the absorber consisting of a wire net made of soft steel ("V"-corrugated porous absorber). Both types of absorbers are painted black, to convert the maximum amount of solar energy into heat.

Figure 4: "U"-corrugated absorber (left) and V-corrugated porous absorber (right).

The collector based on the V-corrugated porous absorber has a rectangular shape. Its casing is made of wood and has the length equal to 1.2 m and width equal to 0.8 m. A sketch of this collector is presented in Figure 5(a). The absorber material is a double-layered wire net of fine meshes, of about 0.1–0.2 mm, which can be seen as a porous material with large pores, of about 0.05–0.1 mm (Figure 5(b)). The wire net is placed in the casing so that the air flows over, under and through the net mesh. From this point of view, the collector can be seen as a combination of a single-passage air collector and a through-pass air collector. The effective surface of the porous absorber made of two wire nets is ($2 \times 0.7 \times 1.523 = 2.1322\,\mathrm{m}^2$). The effective heat transfer area between the wire mesh and air has been calculated with the following formula:

$$A_{ab} = n\left(\left(\frac{W_{ab}}{Pt}\right) \cdot L_{ab} + \left(\frac{L_{ab}}{Pt}\right) \cdot W_{ab}\right) \cdot \pi \cdot Th_{ab} \tag{1}$$

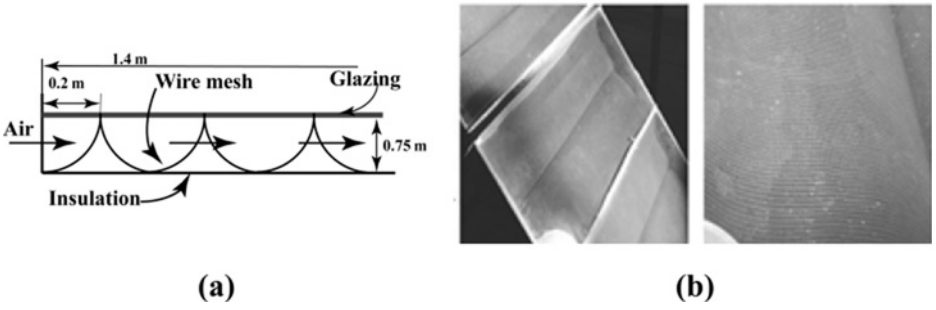

Figure 5: (a) Sketch of the solar collector based on V-corrugated porous absorber and (b) view of the V-porous absorber.

where W_{ab} is the width of one steel mesh (0.7 m), L_{ab} is the length of one steel mesh (1.523 m), Pt is the pitch of the steel mesh (0.00017 m), Th_{ab} is the diameter of the steel mesh wire (0.0001 m) and n is the number of wire nets ($n = 2$; double-layered wire net). After calculations, the effective heat transfer area between the wire mesh and air is found to be 7.88 m^2. Both the "V"-corrugated porous absorber collector and the "U"-corrugated absorber collector have the same net aperture surface area (glass cover area) of 1.125 m^2 (1.5 m × 0.75 m). However, the heat transfer area is larger for the collector with a V-corrugated porous absorber than that of the collector with a U-corrugated absorber.

The collector with "U"-corrugated absorber has three straight baffles to divert the flow and raise the turbulence coefficient (Figure 6(a) and (b)). A gap is maintained between the glass cover and the absorber plate. The air passes through the air channel (under the absorber plate) to collect heat from the absorber, which is an aluminum sheet painted black with a thickness of 0.35 mm. The absorptance and thermal conductivity coefficients of the plate are 95 % and 205 W/(m K), respectively.

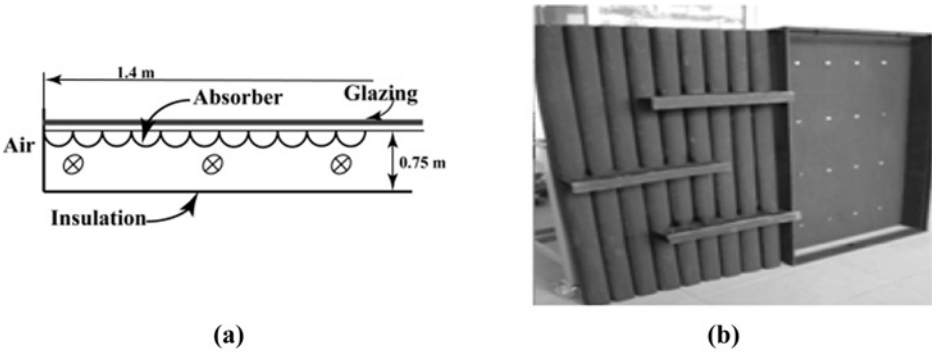

Figure 6: (a) Sketch of the solar collector based on U-corrugated absorber and (b) view of the "U" absorber with baffles.

2.2 Thermal transducers

Thirty-two thermal transducers were used, distributed evenly on the bottom surface of the absorber (see Figure 7), at identical positions along the direction of air flow for each collector. Inlet air temperatures were measured by two thermal transducers. Four thermal transducers were fixed at the end section of each collector to measure the outlet air temperatures. The thermal transducers were mounted in

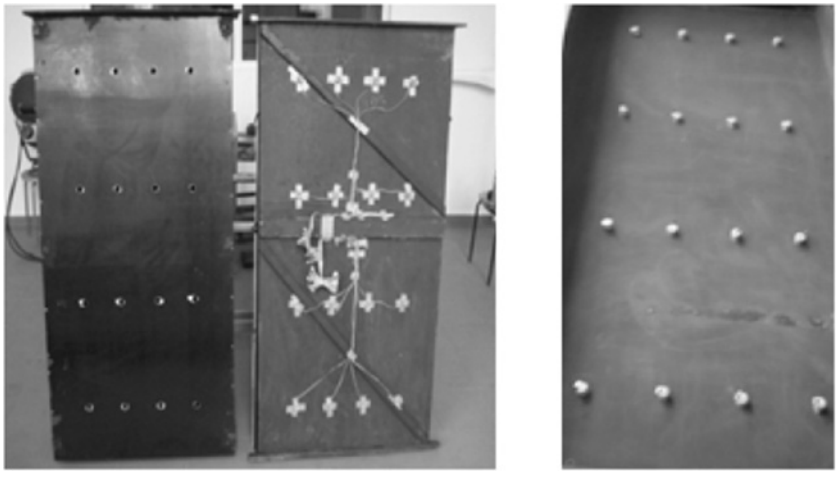

Figure 7: Thermal transducers for both solar thermal air collectors.

the same position in the entrance area of both collectors, in order to obtain the inlet temperature distributions. All thermal transducers were connected to a computer. Measurements were recorded at 10-s time intervals.

3 Analysis of experimental data

The useful heat flux supplied by the collector to the air is computed by using the following equation:

$$\dot{Q}_{\mathrm{u}} = \dot{m}_{\mathrm{a}} Cp_{\mathrm{a}} (T_{\mathrm{a,\,out}} - T_{\mathrm{a,\,in}}) \tag{2}$$

where $(T_{\mathrm{a,\,out}} - T_{\mathrm{a,\,in}})$ is the air Spara temperature increase between collector inlet and outlet and $\dot{m}_{\mathrm{a}}$ (kg/s) is the mass flow rate of air, given by

$$\dot{m}_{\mathrm{a}} = \rho_{\mathrm{a}} \dot{V}_{\mathrm{a}} = \rho v_{\mathrm{a}} \frac{\pi \cdot d^2}{4} \tag{3}$$

where $\dot{V}_{\mathrm{a}}$ is the volumic flow rate of air exiting the collector via the duct of diameter d, v_{a} is the air speed and ρ_{a} is the density of air. The specific heat of air, Cp_{a} [kJ/(kg K)], is assumed to vary linearly with temperature (°C) by [23]

$$Cp_{\mathrm{a}} = 1.0057 + 0.000066(T_{\mathrm{m,\,a}} - 27) \tag{4}$$

The solar energy flux absorbed by the solar collector absorber is given by

$$Q_{\mathrm{s}} = (\tau\alpha) G_{\mathrm{T}} A_{\mathrm{c}} \tag{5}$$

where G_{T} (W/m^2) is the total solar irradiance incident on the tilted collector surface, A_{c} (m^2) is the collector surface area and $(\tau\alpha)$ is the effective transmittance–absorptance product, which is evaluated by using the following equation:

$$(\tau\alpha) = \frac{\tau\alpha}{1 - (1 - \alpha)\rho_g} \tag{6}$$

The thermal efficiency of solar air collectors is defined as the ratio of the useful heat flux supplied by the collector and the total energy flux absorbed by the absorber [24]:

$$\eta = \frac{\dot{m}_{\mathrm{a}} Cp_{\mathrm{a}} (T_{\mathrm{a,\,out}} - T_{\mathrm{a,\,in}})}{A_{\mathrm{c}} (\tau\alpha) G_{\mathrm{T}}} \tag{7}$$

The ambient temperature, the solar irradiance, the outlet air temperature and the outlet air velocity have been measured. The heating characteristic of the collector, the air flow rate, the heat flux and finally the solar energy conversion efficiency into thermal energy were computed.

In steady-state operation conditions, the flux of useful heat delivered by a solar collector is equal to the flux of energy absorbed by the working fluid (the air) minus the flux of heat losses from the absorber surface to the surroundings. The useful output flux of the solar air collectors can be written as

$$Q_u = [(\tau\alpha) G - U_L (T_{\mathrm{ma}} - T_{\mathrm{amb}})] \tag{8}$$

The solar energy flux absorbed by the absorber per unit surface area, S (W/m^2), is calculated by [24]

$$S = (\tau\alpha) G_T \tag{9}$$

The performance of the two collectors has been compared, by using measurement data. The solar air collector with V-corrugated porous absorber is more effective or less effective than the solar air collector with U-corrugated absorber, depending on the radiative regime. For instance, the efficiency of the collector based on V-porous absorber is higher near the noon of clear days. However, in the beginning

and at the end of clear days, the collector based on porous absorber is less effective that the collector with U-corrugated absorber (see Table 2).

Table 2: Efficiency of the collector with V-corrugated porous absorber and V-corrugated absorber, respectively, at different hours during the clear day 22 September 2014.

Time	Solar irradiance G (W/m^2)	V-corrugated porous absorber	U-corrugated absorber
9:00	222	0.150	0.158
10:00	460	0.163	0.150
11:00	791	0.262	0.221
12:00	966	0.545	0.394
13:00	1,118.5	0.621	0.483

4 Models

Two models for unsteady-state operation have been developed; the first one is for the solar air collector with "V"-corrugated porous absorber and the second is for the solar air collector with "U"-corrugated absorber.

The absorber temperature depends on the coordinate in the direction of air flow. Three nodes for each type of solar air collector have been considered (i. e. the mean value of temperature in glass cover, absorber and flowing air, respectively). The governing equations are obtained by applying the energy balance for each node. The energy balance equations are written under the following assumptions:

- There is no temperature gradient along the thickness of the glass cover.
- The air does not absorb solar radiation.
- Thermal losses through the collector backs and sides are mainly due to conduction across the wood (3 cm thickness) and those caused by wind and thermal radiation are neglected.
- The air flow properties depend on temperature.
- The inlet air temperature is equal to the ambient temperature.
- All air channels are assumed to be free of leakage.
- The collectors are facing south (toward the midday sun in Bucharest).

4.1 Time-dependent model of the solar air collector with "V"-corrugated porous absorber

The energy input to the solar collector comes from the solar radiation received on the absorber surface. The solar radiation is transmitted from the glass cover and is absorbed by the absorber. The air flows through the porous absorber, where it is heated. The set of equations can be illustrated using thermal networks. The model consists of three nodes corresponding to the glass cover, air flow and mesh absorber, respectively. Details are as follows.

4.1.1 Glass cover

The small thickness of the cover makes it reasonable to assume that the properties of the glass are constant and thereby consider a uniform temperature throughout it. Convection heat transfer occurs between the glass and the ambient and radiation is coming to the glass from the sun and from the absorber. The change

of the internal energy of the glass cover equals the absorbed energy from the sun plus the energy transferred by convection and radiation from the absorber minus the outgoing energy by convection to the ambient minus the outgoing energy through radiation to the sky (see eq. [12] in Appendix A).

4.1.2 Working fluid (air)

The thermal energy gained by the air in the collector is equal to the heat flux transferred from the wire mesh absorber to the air minus the heat transferred from the air flow to the glass cover minus the net thermal energy transported by the air flow out of the collector (see eq. [13] in Appendix A).

4.1.3 Mesh absorber

The change of the internal energy of the wire mesh absorber equals the absorbed energy from the sun minus the thermal energy transferred by convection to the glass minus the radiative heat transfer from the absorber to the glass cover (see eq. [14] in Appendix A).

4.2 Time-dependent model of the solar air collector with "U"-corrugated absorber

The other solar air collector consists of the glass cover, the absorber and a flat wooden bottom that is attached by the back insulation underneath. The space between the "U"-corrugated absorber and the wooden bottom is the air flow channel, in which air is heated by the solar radiation absorber. The air flows along the U-corrugated absorber. A system of three differential equations was derived to describe the energy balance of the glass, air and absorber plate, respectively. Details are as follows.

4.2.1 Glass cover

The small thickness of the cover makes it reasonable to consider a uniform temperature throughout it. Heat is transferred by conduction from the glass to the ambient and from the absorber to the glass and by radiation from the sun and absorber, respectively, to the glass. One denotes by $h_{c,p\text{-}g}$ (W/m^2 K) the convection heat transfer coefficient between the absorbing plate and the glass cover, by $h_{r,p\text{-}g}$ (W/m^2 K) the radiation heat transfer coefficient between the absorbing plate and the cover, by $h_{c,g\text{-}amb}$ (W/m^2 K) the convection heat transfer coefficient between the glass cover and the ambient and by $h_{r,g\text{-}sky}$ (W/m^2 K) the radiation heat transfer coefficient between the cover and the sky. The energy balance in the glass cover is given by eq. (15) in Appendix A.

4.2.2 Working fluid (air)

The energy balance can be expressed similarly for the air flowing inside the collector channel and represents the change in the thermal capacity of air over time (see eq. [16] in Appendix A). The right-hand side is equal to the heat exchange between the absorber plate and the air flowing through the collector minus the quantity of heat withdrawn from the collector by the air flow rate.

4.2.3 Absorber plate

The energy balance equation involves the change in the absorber plate thermal capacity over time. It is equal to the input solar energy flux absorbed by the absorber minus the thermal energy flux transferred by

convection from the absorber plate to the air and minus the radiative heat flux and convection heat flux, respectively, transferred from the absorber to the glass cover (see eq. [17] in Appendix A).

4.3 Space-dependent models

For air flowing through the air channel above the thermal transducers, on the bottom surface of the absorber plates (see Figure 7), the steady-state energy balance equation is written for a specific position on the channel (see eq. [18] in Appendix A). The convection heat transfer between the flowing air and the glass cover is considered, together with the heat transferred between the absorber plate and the air.

5 Model solution procedure

The initial temperature distribution in the components of the collector is needed when solving the sets of three first-order differential equations presented in Sections 4.1 and 4.2, respectively. The instantaneous boundary conditions, including solar irradiance, ambient temperature and the mass flow rate of the working fluid (air), should be also known.

The model has four input parameters, namely ambient temperature, solar irradiation, inlet temperature and wind velocity. The collector properties are also inputs for the model. All these parameters are read from the input data files. The models calculate the outlet temperature and compare it with the measured outlet temperature. In addition, the models calculate the absorber temperature, glass cover temperature, mean air temperature and the thermal efficiency of the collectors.

The system of three first-order differential equations was solved by using the Runge–Kutta fourth-order method. The software package used to code the model is MATLAB version R2012a.

6 Models validation

The models were validated by comparing the simulation results with measured data. The experiments were undertaken simultaneously for both solar air collectors, in Bucharest, during September and October 2014. Figure 8 shows the time variation of solar irradiance and ambient temperature during 3 days.

These two collectors were tested in the same experimental facility and under the same meteorological conditions. Thus, the comparison is considered to be a true assessment of the performance. The experiments show that most of the time the collector based on the V-corrugated porous absorber is more effective than the collector based on the “U”-corrugated absorber. The air flow passing throughout the holes of the porous collector contributes to increase the heat transfer surface area per unit volume and, therefore, to increase the thermal efficiency, in comparison with the “U”-corrugated collector. The efficiency of the collector based on V-corrugated porous absorber is higher near the noon of the clear days while in the beginning and at the end of the clear days, the collector based on V-corrugated porous absorber is less effective than the collector with U-corrugated absorber (see Table 2). This may be explained in part by the lower optical efficiency of the porous absorber at large incidence angles, due to the cylindrical shape of the mesh fibers.

Measurement and simulation results for the glass temperature, absorber temperature, ambient temperature and outlet air temperature are shown in Figure 9. Generally, the simulated values follow the same trend as the measured values. The deviation from the measured temperature is larger at the start of the experiments and later on it becomes smaller. For instance, the difference between the simulated and measured outlet air temperature for the collector with V-corrugated porous absorber is about −7° in

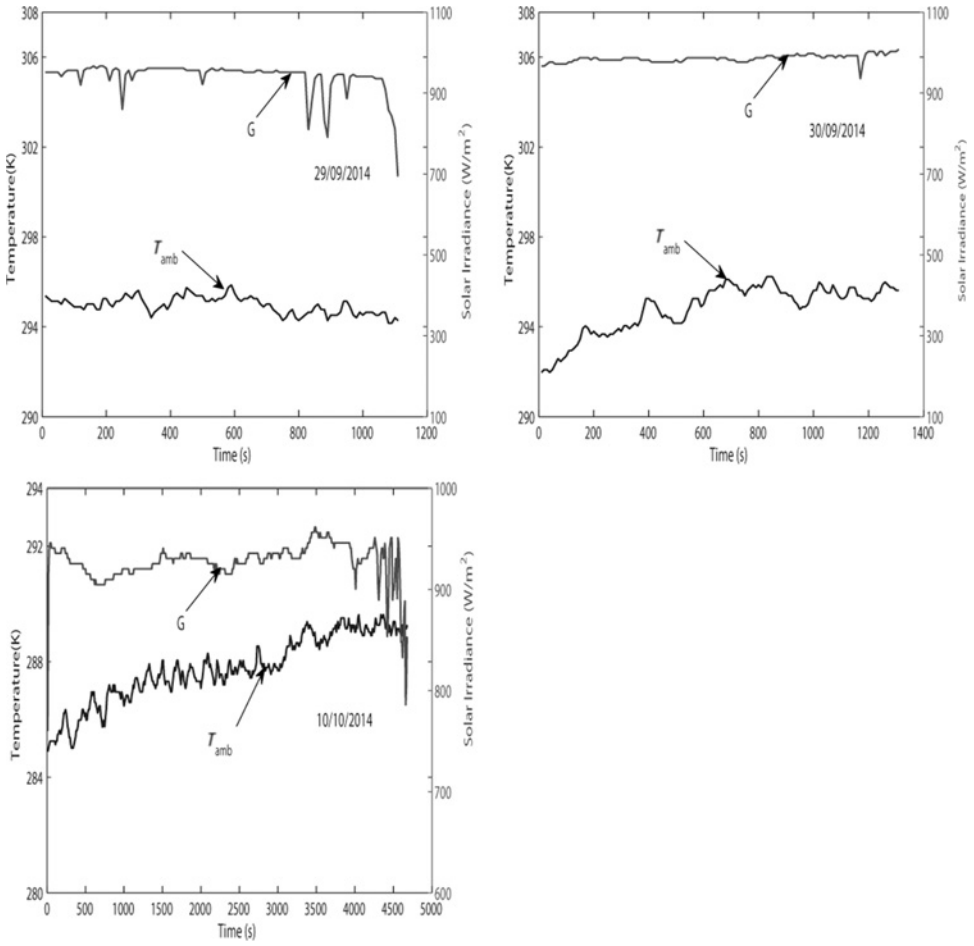

Figure 8: Variation of ambient temperature and solar irradiance during 3 days in Bucharest, Romania.

the early morning of 29 September 2014 but reduces to nearly 0° after 7 min of operation (Figure 9). Rather similar results were obtained for the same collector on 10 October 2014. The initial large difference between simulations and measurements is explained by the thermal inertia of the collector, which is stronger when the air flow starts. Similar results are obtained in case of the collector with U-corrugated absorber, but in that case, the initial simulated temperature is higher than the measured temperature (see Figure 9). Also, the time interval needed for the difference between the simulated and measured temperature to become nearly 0 is about 18 min (see results for 10 October 2014). This may be explained in part by the larger thermal inertia the collector based on U-corrugated absorber than that of the collector based on V-corrugated porous absorber.

Two statistical indicators, namely the relative root mean square error (rRMSE) and the relative mean bias error (rMBE), were used to assess the model performance. They are defined as follows:

$$\mathrm{rRMSE} = \frac{\sqrt{\sum_{i=1}^{n} (C_i - M_i)^2 / n}}{1/n \sum_{i=1}^{n} M_i} \tag{10}$$

$$\mathrm{rMBE} = \frac{\sum_{i=1}^{n} (C_i - M_i)}{\sum_{i=1}^{n} M_i} \tag{11}$$

where C_i and M_i are the calculated and measured values, respectively, and n is the number of observations.

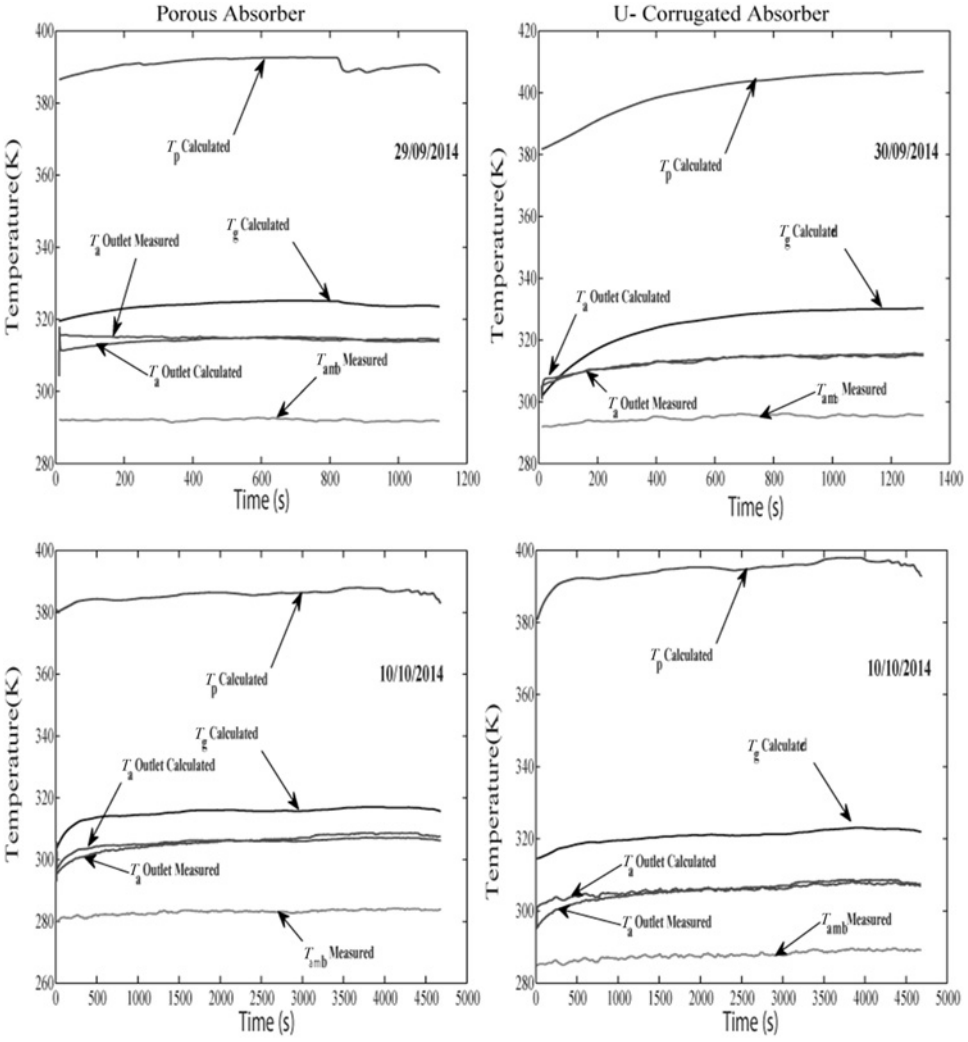

Figure 9: Time variation of several calculated and measured temperatures during days in September and October 2014. Collectors based on both V-corrugated porous absorber and U-corrugated absorbers are considered. The air flow rate is 0.33 kg/s.

Results are presented in Table 3. There is good agreement between simulation results and measurements. Generally, the model developed for the collector based on the U-corrugated absorber works slightly better than that of the collector based on the V-corrugated porous absorber.

Table 3: Comparison between simulation results and measurements.

Statistical indicators	"V"-corrugated porous absorber				"U"-corrugated absorber			
	$T_{a,mean}$	$T_{a,out}$	Q_u	η	$T_{a,mean}$	$T_{a,out}$	Q_u	η
Rrmse	0.0400	0.0042	0.1034	0.1036	0.0147	0.0044	0.0084	0.0843
rMBE	−0.0390	−0.0120	−0.0029	0.0024	−0.0144	0.0007	0.0014	0.0014

It is interesting to compare the results obtained by using the simple steady-state model eq. (8) and the results obtained by using the model based on time-dependent differential equations, proposed in this

paper. Eq. (8) has been used in the following way. Constant values have been used during the day for the optical efficiency $(\tau\alpha)$ and for the overall heat loss coefficient U_L. Next, experimental values during 29 September were used for solar irradiance G, ambient temperature T_{amb} and useful heat flux $\dot{Q}_u$, respectively. Thus, eq. (8) was solved in the only unknown temperature T_{ma}. Figure 10 shows the value of the mean air temperature T_{ma} obtained by this procedure based on the steady-state eq. (8) (which is denoted "measured") and the value T_{ma} obtained by using the model proposed in this paper (which is denoted "calculated"). Both series of temperature T_{ma} are associated with the beginning of the operation and correspond to a constant air mass flow rate 0.33 kg/s. Generally, the steady-state model provides temperature values smaller by a few degrees than the dynamic model. The steady-state model works better in case of the collector based on a V-corrugated porous absorber.

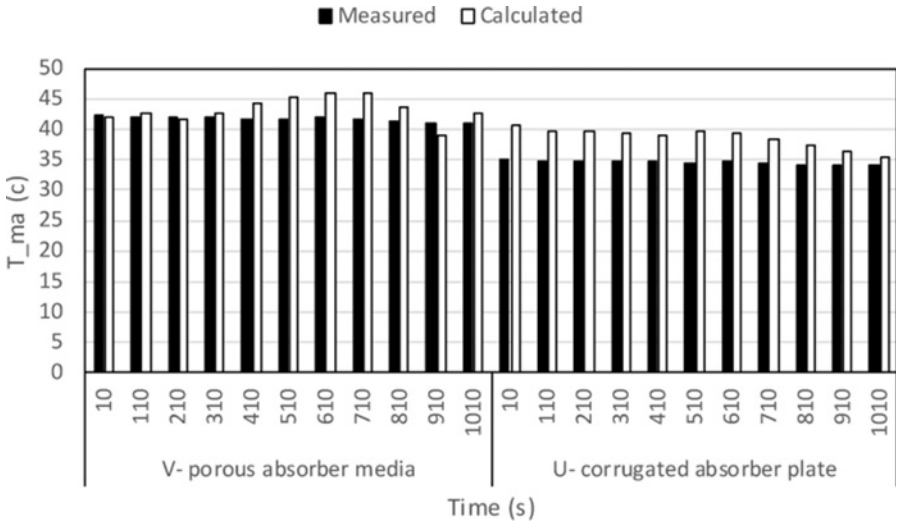

Figure 10: Mean air temperature T_{ma} obtained by using the steady-state eq. (8) (denoted "measured") and the models proposed in this paper (denoted "calculated") for both solar air collectors. Results correspond to the beginning of the operation. A constant air mass flow rate 0.33 kg/s has been considered on 29 September 2014.

Note that in order to provide the same conditions for the air motion in both collectors (i. e. the same energy consumption, when the same mass flow rate is provided in both collectors), a metal network was placed at the inlet section of the collector with U-corrugated absorber. The network characteristics were the same as the ones used in the collector with V-corrugated porous absorber. By adding a number of metal network sheets and by monitoring the power consumption of the fans, one obtains the same flow conditions for the internal air motion, or, in other words, the same pressure losses across both collectors. Moreover, for both collectors, pressure losses were monitored by pressure transducers placed at the same distance from the outlet (see Figure 3).

The mass flow rate is included in the models as an input parameter but the energy needed to generate this mass flow is not considered in the energy balance and efficiency calculations. The use of a porous material would indeed enhance the thermal coefficients and thus would raise the efficiency of the solar collectors. However, this would also increase the drag force such that more energy may be required to maintain the constant mass flow rate, which leads to a decrease of the efficiency.

It is useful to estimate the approximation induced by neglecting the energy needed to move the air inside the collectors. We have selected a time period of 20 min starting at 12 pm hour on 29 September. The useful heat collected by the collector based on the porous absorber is 604,052 J. The fan power is 18 W. During a 20-min interval, the electrical energy consumed by the fan is 21,600 J (electrical energy).

This energy is 21,600/604,052 = 3.57 % of the useful thermal energy provided by the air solar collector. To find how much thermal energy is consumed into a power plant to produce this amount of electrical energy, one multiplies the value of the electrical energy by 3.5, which is the average performance factor for the power plants in Romania. The result is 75,600 J (thermal energy). This thermal energy is 75,600/604,052 = 12.5 % of the useful thermal energy provided by the air solar collector. Therefore, neglecting the electrical energy needed to vehiculate the air in the collector is a quite reasonable assumption.

A typical space distribution of the air temperature along the air channels is shown in Figures 11 and 12 for both types of solar air collectors, for two irradiance levels. Average air temperatures were computed for the four lines of thermal transducers. The average temperature is a function of the position inside the air channel (four positions were considered here, namely $X_1 = 19.5$ cm, $X_2 = 56.5$ cm, $X_3 = 93.5$ cm and $X_4 = 140.5$ cm, as shown in Figure 3).

The average air temperature increases as the air is moving along the air channel, as expected. Also, the average temperatures exhibit a slight tendency to decrease near to the air heater outlet. This tendency was attributed to the end divergence and cooling effects and to mixing of the outgoing hot air with the ambient air due to recirculation.

In most experiments, the temperature variation across the collector is less than 5° for both collectors. However, this temperature variation can be as high as 10° in the V-corrugated porous collector at high values of the incident radiation (Figure 11). The model is based on the average temperature inside the collector. Thus, the underestimation at collector inlet is well compensated by the overestimation at collector outlet, as shown by the good agreement between the computed and the experimental results (see Table 3).

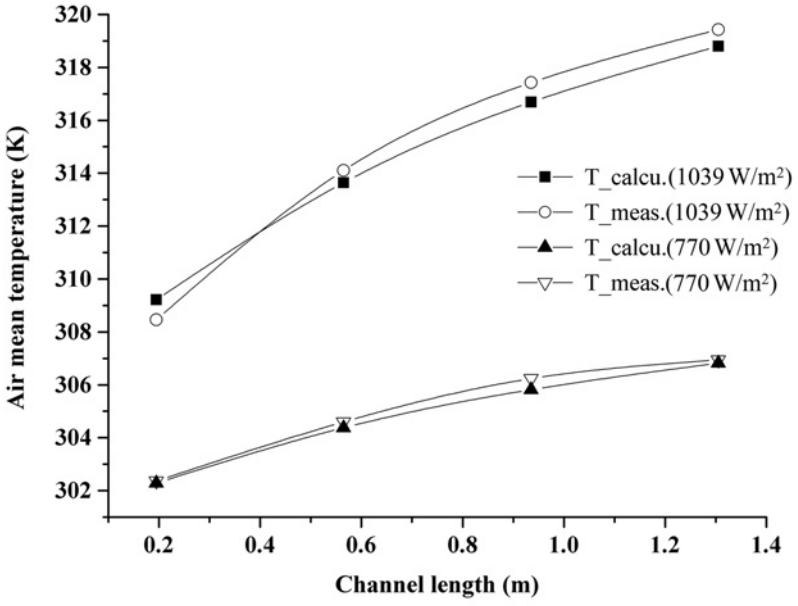

Figure 11: Space variation of the average air temperature in the collector with "V"-corrugated porous absorber.

Notice that the temperature difference between the average measured temperature and the average temperature calculated by eq. (18) (in Appendix A) is between 1.5 and 2°. The air temperature variation is

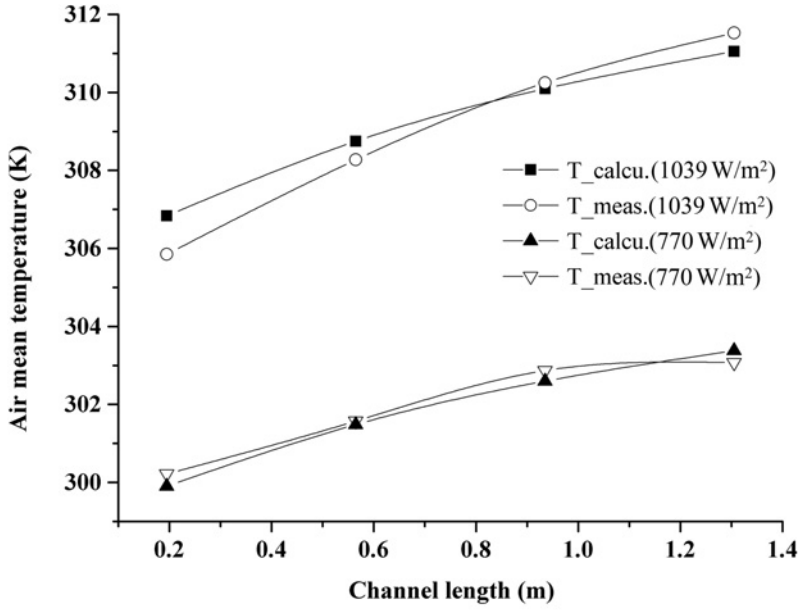

Figure 12: Space variation of the average air temperature in the collector with "U"-corrugated absorber.

affected by the absorber type and by the level of the solar irradiance. Figures 11 and 12 show that the temperature tends to increase with increasing solar irradiance.

7 Conclusions

The operation of solar air collectors in real-world conditions, involving fluctuating incident solar irradiance, is inherently dynamic. Explicit time-dependent models of solar air collectors with and without porous absorber, suitable for dynamic system simulation, have been presented. Two specific air heaters have been considered: a V-corrugated porous collector and a "U"-corrugated collector. Note that V-corrugated absorbers have been treated in previous papers but the V-corrugated porous absorbers modeled here have not been very often considered in literature. A series of experiments have been performed under different weather conditions in Bucharest, Romania.

The results show that there is good agreement between the theoretical results and experiments. The rRMSE was about 10.36 % and 8.43 % for the solar air collectors with "V"-corrugated porous absorber and "U"-corrugated absorber, respectively.

An experimental comparison of the thermal performances of the two collectors was carried out under a wide range of configurations and operating conditions. The collector based on V-corrugated porous absorber has higher efficiency than the collector with U-corrugated absorber in the middle of clear days. Around sunrise and sunset the collector with U-corrugated absorber is more effective.

Acknowledgements: The authors thank the reviewers for useful comments and suggestions. One author (QAA) thanks the Ministry of Higher Education of Iraq for financial support during the preparation of this work.

Appendix A: Energy balance equations

Model of solar air collector with "V"-corrugated porous absorber

– **Glass cover**

$$M_g Cp_g \frac{dT_g}{dt} = \begin{bmatrix} \alpha_g G A_c + h_{c,a-g} A_{ab}(T_{ma} - T_g) + h_{r,p-g} A_{ab}(T_p - T_g) \\ - h_{c,g-amb} A_c (T_g - T_{amb}) - h_{r,g-sky} A_c (T_g - T_{sky}) \end{bmatrix} \tag{12}$$

– **Working fluid (air)**

$$M_a Cp_a \frac{dT_a}{dt} = \begin{bmatrix} h_{c,p-a} A_{ab}(T_p - T_{ma}) - h_{c,a-g} A_{ab}(T_{ma} - T_g) \\ - m_a Cp_a (T_{a,out} - T_{a,in}) \end{bmatrix} \tag{13}$$

– **Mesh absorber**

$$M_p Cp_p \frac{dT_p}{dt} = \left[(\tau\alpha) G A_c - h_{c,p-a} A_{ab}(T_p - T_{ma}) - h_{r,p-g} A_{ab}(T_p - T_g) \right] \tag{14}$$

Model of solar air collector with "U"-corrugated absorber

– **Glass cover**

$$M_g Cp_g \frac{dT_g}{dt} = \begin{bmatrix} \alpha_g G A_c + h_{c,p-g} hc_{p-g} A_{ab}(T_p - T_g) + h_{r,p-g} A_{ab}(T_p - T_g) \\ - h_{c,g-amb} A_c (T_g - T_{amb}) - h_{r,g-sky} A_c (T_g - T_{sky}) \end{bmatrix} \tag{15}$$

– **Working fluid (air)**

$$M_a Cp_a \frac{dT_{ma}}{dt} = \left[h_{c,p-a} A_{ab}(T_p - T_{ma}) - \dot{m}_a Cp_a (T_{a,out} - T_{a,in}) \right] \tag{16}$$

– **Absorber plate**

$$M_p Cp_p \frac{dT_p}{dt} = \begin{bmatrix} (\tau\alpha) G A_c - h_{c,p-a} A_{ab}(T_p - T_{ma}) - h_{r,p-g} A_{ab}(T_p - T_g) \\ - h_{c,p-g} A_{ab}(T_p - T_g) \end{bmatrix} \tag{17}$$

Space-dependent models

$$M_a Cp_a \frac{dT_a}{dx} = \left[h_{c,p-a} A_{ab}(T_p - T_a) - h_{c,a-g} A_{ab}(T_a - T_g) \right] \tag{18}$$

Appendix B: Determination of heat transfer coefficients

The heat transfer coefficients by convection from the glass cover due to wind is [25]

$$h_{c,g-amb} = 5.7 + 3.8 v_{wind} \tag{19}$$

The radiation heat transfer coefficient from glass cover to sky is [26]

$$h_{r,g-sky} = \sigma \varepsilon_g (T_g + T_{sky}) \left(T_g^2 + T_{sky}^2 \right) \tag{20}$$

The sky is considered as a black body at some fictitious sky temperature, T_{sky}. Since the sky temperature is a function of many parameters, it is difficult to make a correct estimate of it. Investigators have estimated it using different correlations. One widely used equation due to [24] for clear sky is

$$T_{sky} = T_{amb} - 6 \tag{21}$$

The mean air temperature is calculated as the average between air temperatures at inlet and outlet of the collector:

$$T_{ma} = \frac{T_{a,out} + T_{a,in}}{2} \tag{22}$$

In the porous absorber, the Nusselt number for the convection coefficient, from the air to glass cover, in the case of Reynolds number and Prandtl number $5 \times 10^5 < Re_a < 10^7$ and $0.5 < Pr_a < 2{,}000$, respectively, is [27]

$$Nu_{a-g} = \sqrt{\left(0.664 \cdot Re_a^{0.5} \cdot Pr_a^{1/3}\right)^2 + \left(\frac{0.073 Re_a^{0.8} Pr_a}{1 + 2Re_a^{-0.1}\left(Pr_a^{2/3} - 1\right)}\right)^2} \tag{23}$$

For $Pr_a \leq 0.05$,

$$Nu_{a-g} = 0.565 \cdot \sqrt{Re_a \cdot Pr_a} \tag{24}$$

For other values of the Prandtl number,

$$Nu_{a-g} = 0.0296 \cdot \sqrt{Re_a^{4/5} \cdot Pr_a^{1/3}} \tag{25}$$

The most important heat transfer relation is between the absorber and the air flow. Forced convection is the predominant mode of heat transfer. The equation of the Nusselt number for the wire mesh developed by [28] is

$$Nu_{p-a} = \begin{bmatrix} 4 \times 10^{-4} (Re_a)^{1.22} \left(\frac{P_t}{D_h}\right)^{0.625} \left(\frac{s}{10P_t}\right)^{2.22} \left(\frac{1}{10P_t}\right)^{2.66} \\ \exp\left[-1.25\left(\ln\frac{s}{10P_t}\right)^2\right] \exp\left[-0.824\left(\ln\frac{l}{10P_t}\right)^2\right] \end{bmatrix} \tag{26}$$

Also, the Nusselt number to calculate the convection heat transfer between the "U"-corrugated plate to air, in the case of laminar flow ($Re_a < 2{,}300$), [29] is

$$Nu_{p-a} = 5.4 + \frac{\left(0.0019 \times \left(Re_a Pr_a \left(\frac{D_h}{L}\right)\right)^{1.71}\right)}{\left(1 + 0.00563 \times \left(Re_a Pr_a \left(\frac{D_h}{L}\right)\right)^{1.71}\right)} \tag{27}$$

For transitional flow ($2{,}300 < Re_a > 6{,}000$) [15],

$$Nu_{p-a} = 0.116 \times (Re_a)^{2/3} - 125 \times Pr_a^{1/3} \times \left(1 + \left(\frac{D_h}{L}\right)^{2/3} \times \left(\frac{\nu_a}{\nu_w}\right)^{0.14}\right) \tag{28}$$

For turbulent flow ($6{,}000 < Re_a$, $10 < L/D_h < 400$),

$$Nu_{p-a} = 0.036 \times (Re_a)^{0.8} \times Pr_a^{1/3} \times (D_h/L)^{0.055} \tag{29}$$

The flow characteristics in forced convection are generally described by the Reynolds number:

$$Re_a = \frac{\nu_a L}{\mu_a} \tag{30}$$

The convection heat transfer coefficient for the air moving inside the air channel is

$$h_{c,p-a} = \frac{Nu_a k_a}{D_h} \tag{31}$$

The radiation heat transfer coefficient between the glass cover and the absorber for both types of collectors is calculated by

$$h_{r,p-g} = \frac{\sigma\left(T_p + T_g\right)\left(T_p^2 + T_g^2\right)}{\left(\frac{1}{\varepsilon_p}\right) + \left(\frac{1}{\varepsilon_g}\right) - 1} \tag{32}$$

References

[1] D. Dovic and M. Andrassy, Numerically assisted analysis of flat and corrugated plate solar collectors thermal performances, *J. Solar Energy* **86** (2012), 2416–2431.

[2] N. Hitesh Panchal, N. Soni, M. Prajapti, D. Patel, U. Soni, J. Prajapti, et al., Experimental investigation on double pass air heater with corrugated absorber plate and amul cool aluminum cans, *Int. J. Adv. Eng. Technol*. **11** (2011), 324–328.

[3] M. Varun, R. Saini and S. Singal, A review on roughness geometry used in solar air heaters, *J. Solar Energy* **81** (2007), 1340–1350.

[4] A. Lanjewar, J. Bhagoria and R. Sarviya, Heat transfer and friction in solar air heater duct with W-shaped rib roughness on absorber plate, *J. Energy*. **36** (2011), 4531–4541.

[5] H. Chii-Dong, H.,Y. Ho-Ming and C. Tsung-Ching, Collector efficiency of upward-type double-pass solar air heaters with fins attached, *Int. Commun. Heat Mass Transfer* **38** (2011), 49–56.

[6] M. Yang, X. Yang, X. Li, Z. Wang and P. Wang, Design and optimization of a solar air heater with offset strip fin absorber plate, *Appl. Energy* **113** (2014), 1349–1362.

[7] M. Sabzpooshani, K. Mohammadi and H. Khorasanizadeh, Exergetic performance evaluation of a single pass baffled solar air heater, *Energy* **64** (2014), 697–706.

[8] W. Chang, Y. Wang, M. Li, X. Luo, S. Zhang, Y. Ruan, et al., The theoretical and experimental research on thermal performance of solar air collector with finned absorber, *Energy Procedia* **70** (2015), 13–22.

[9] S. Gurpreet and S. Sidhu, Enhancement of heat transfer of solar air heater roughened with circular transverse RIB, *Int. Adv. Res. J. Sci. Eng. Technol*. **1** (2014), 196–200.

[10] W. Gao, W. Lin and E. Lu, Numerical study on natural convection inside the channel between the flat-plate cover and sine-wave absorber of a cross-corrugated solar air heater, *Energy Convers. Manage*. **41** (2000), 145–151.

[11] W. Lin, W. Gao and T. Liu, A parametric study on the thermal performance of cross-corrugated solar air collectors, *Appl. Therm. Eng*. **26** (2006), 1043–1053.

[12] W. Gao, W. Lin, T. Liu and C. Xia, Analytical and experimental studies on the thermal performance of cross-corrugated and flat-plate solar air heaters, *Appl. Energy* **84** (2007), 425–441.

[13] M. Karim, E. Perez and Z. Amin, Mathematical modelling of counter flow V-grove solar air collector, *J. Renewable Energy* **67** (2014), 192–201.

[14] M. Fakoor Pakdaman, A. Lashkari, H. Basirat Tabrizi and R. Hosseini, Performance evaluation of a natural-convection solar air-heater with a rectangular-finned absorber plate, *Energy Convers. Manage*. **52** (2011), 1215–1225.

[15] L. Tao, L. Wenxian, G. Wenfeng and X. Chaofeng, A comparative study of the thermal performances of cross-corrugated and V-groove solar air collectors, *Int. J. Green Energy* **4** (2007), 427–451.

[16] A. Anuradha and R. Oommen, Fabrication and performance evaluation of a v-groove solar air heater, *Int. J. Sci. Eng. Res*. **4** (2013), 2072–2080.

[17] N. Paisarn and K. Bancha, Theoretical study on heat transfer characteristics and performance of the flat-plate solar air heaters, *Int. Commun. Heat Mass Transfer* **30** (2003), 1125–1136.

[18] M. El-Khawajah, F. Egelioglu and M. Ghazal, Finned single-pass solar air heaters with wire mesh as an absorber plate, *Int. J. Green Energy* **12** (2015), 108–116.

[19] K. Sopian, Supranto, W. Daud, M. Othman and B. Yatim, Thermal performance of the double-pass solar collector with and without porous media, *Renewable Energy* **18** (1999), 557–564.

[20] D. Munuswamy, V. Madhavan and M. Mohan, Comparison of the effects of Al_2O_3 and CuO nanoparticles on the performance of a solar flat-plate collector, *J. Non-Equilib. Thermodyn*. **4** (2015), 265–273.

[21] V. Madadi, H. Beheshti, T. Tavakoli and A. Rahimi, Experimental study and first thermodynamic law analysis of a solar water heater system, *J. Non-Equilib. Thermodyn*. **40** (2015), 171–183.

[22] D. Munuswamy and V. Madhavan, Experimental analysis on the influence of internal finning on the efficiency of solar flat plate collector using Al_2O_3 nanoparticles, *J. Non-Equilib. Thermodyn*. **40** (2015), 185–192.
[23] K. S. Ong, Thermal performance of solar air heaters: mathematical model and solution procedure, *Sol. Energy* **55** (1995), 93–109.
[24] J. A. Duffie and W. A. Beckman, *Solar Engineering of Thermal Processes*, 2nd ed., John Wiley & Sons, New York, 1991.
[25] W. H. McAdams, *Heat Transmission*, 3rd ed., McGraw-Hill, New York, 1954.
[26] X. Zhai, Y. Dai and R. Wang, Comparison of heating and natural ventilation in a solar house induced by two roof solar collectors, *Appl. Thermal Eng*. **25** (2005), 741–757.
[27] VDI-Gesellschaft, *Verfahrenstechnik Und Chemieingenieurwesen, VDI Heat Atlas*, Springer Heidelberg, Dordrecht, London, New York, 2010.
[28] R. Saini and J. Saini, Heat transfer and friction factor correlation for artificially roughened ducts with expanded metal mesh as roughness element, *Int. J. Heat Mass Transfer* **40** (1997), 973–986.
[29] B. Benamar and S. Rachid, Theoretical investigation of finned and baffled flat plate single-pass solar air heaters with and without glass cover. 1st National Conference on Renewable Energy and Applications, 2014.